Clays and Clay Minerals, Vol. 65, No. 1, 1–13, 2017.

DENSITY FUNCTIONAL THEORY COMPUTATION OF ORGANIC COMPOUND PENETRATION INTO SEPIOLITE TUNNELS

DENIZ KARATAŞ[1], ADEM TEKIN[2,*], AND MEHMET SABRI ÇELIK[1]

[1] Istanbul Technical University, Mineral Processing Engineering Department, 34469 Maslak, Istanbul, Turkey
[2] Informatics Institute, Istanbul Technical University, 34469 Maslak, Istanbul, Turkey

Abstract—Sepiolite is a fibrous clay mineral and consists of 2:1 silicate blocks connected at the corners and separated by tunnels (channels on external surfaces) that extend in the direction of fiber length. The tunnels, 3.7 Å × 10.6 Å in cross-section, are responsible for the incorporation of organic and inorganic compounds. The present study aimed to examine the capacity of twelve different organic molecules, such as pyridine, indigo, methylene blue, and quaternary amines, to gain access to the tunnels of sepiolite using quantum chemistry techniques. The interaction energy computations performed at the B97-D/TZVP level showed that all of the considered organic molecules tend to access the tunnels of sepiolite if external water molecules are absent. This finding is in agreement with experimental studies that included pyridine, indigo, 2,2-bipyridyl, and methylene blue. Interestingly, 2,6-dimethyl pyridine preferred to remain in a tunnel rather than an external channel of the sepiolite.

Key Words—Binding Energy, Cavity, Density Functional Theory, Host-guest Complex, Indigo, Methylene Blue, Organic-inorganic Hybrid Material, Pyridines, Quantum Chemical Computation, Sepiolite Tunnel, Quaternary Ammonium Compounds

INTRODUCTION

Porous materials, such as natural clay minerals, find widespread use in many technological applications that range from gas storage to drug delivery. The features of the pores, such as size, shape, and volume, have a direct influence on performance for a desired function in a particular application (Davis, 2002). In addition to the pore characteristics, the atoms that appear in the pore are also important for specific applications. For instance, hydrophobic or hydrophilic pores can allow the adsorption of organic compounds or water. The incorporation of organic compounds in cavities is a challenging task that leads to unusual properties in nanotechnologies and microtechnologies (Ovarlez *et al*., 2009). The resulting organic-inorganic hybrid materials attract particular attention among researchers (Mehdi *et al*., 2011) and numerous materials have found potential applications in a number of fields, such as optics, electronics, mechanics, membranes, catalysis, sensors, and biology (Mammeri *et al*., 2005).

Sepiolite with the formula $Si_{12}Mg_8O_{30}(OH)_4(H_2O)_4{\cdot}8H_2O$ is one of the interesting porous clay minerals, which has channels and tunnels. The penetration of several organic compounds into sepiolite intracrystalline cavities was examined in the published literature. In particular, some polar molecules, such as ammonia, methanol, acetone (Kuang *et al*., 2006), and ethylene glycol reportedly can be incorporated into the tunnels of sepiolite (Ruiz-Hitzky, 2001). Ruiz-Hitzky (2001) also indicated that slightly larger molecules like hexane and benzene can access the cavities of sepiolite. Moreover, Ruiz-Hitzky (2001), Ovarlez *et al.* (2009), and Sabah and Çelik (2002) showed that much larger compounds like pyridine, methylene blue, indigo, and 2,2-bipyridyl can also penetrate into the structural pores of sepiolite. Spectroscopic studies by Guistetto *et al*. (2010, 2011b) also supported the findings of Ovarlez *et al*. (2009), which indicated that indigo can be encapsulated inside a sepiolite tunnel. Furthermore, Ruiz-Hitzky (2001) also indicated that a pyridine derivative, 2,6-dimethylpyridine, cannot access the pores of sepiolite and instead accumulates in the channels. In addition to these experimental studies, a few computational studies were also carried out to explain the penetration of organic compounds into the tunnels of sepiolite. More specifically, a molecular dynamics study by Guistetto *et al*. (2011a) indicated that indigo can be accommodated in the tunnels. The density functional theory (DFT) computations of Alvarado *et al*. (2012) showed that the indigo molecule can be inserted into the channels of sepiolite.

Quantum chemical computations are extremely useful tools to investigate systems at the atomic level. Only a few such studies that focussed on the incorporation of organic molecules into the tunnels of sepiolite, however, were found. In the present study, this phenomenon was, therefore, systematically investigated with the help of DFT and using the organic compounds pyridine, 2,5-dimethylpyridine, 2,6-dimethylpyridine, 2,2-bipyridyl, 3,3-bipyridyl, lauric acid (*i.e*. dodecanoic acid), indigo, methylene blue, distearyldimethylammonium chloride

* E-mail address of corresponding author:
adem.tekin@be.itu.edu.tr
DOI: 10.1346/CCMN.2016.064043

(DDAC), hexadecyltrimethylammonium chloride (HTAC), stearyldimethylbenzylammonium chloride (SDBAC), and tetradecyldimethylethylbenzylammonium chloride (TDEBAC), most of which have been considered in experimental studies. This selection of organic compounds will certainly provide an opportunity to compare the results of the present study with published experimental studies and understand why some of the compounds can access the tunnels and some cannot. Computations involved in the present study basically included two types of host-guest interactions: i) static and ii) dynamic. Static host-guest interactions are used for organic compounds that were initially placed inside a sepiolite tunnel, whereas in dynamic host-guest interactions, the paths of organic compounds that enter a sepiolite tunnel are considered.

COMPUTATIONAL DETAILS

The tunnel model of sepiolite (Figure 1) was prepared using a published sepiolite crystal structure (Post *et al*., 2007). A tunnel with an approximate size of 7.4 Å × 10.6 Å × 16.5 Å is large enough to enclose all of the considered organic molecules. All dangling bonds in this tunnel model were saturated with hydrogen, which is similar to what was used in other studies (Chatterjee *et al*., 1997; Chatterjee *et al*., 1999; Tunega *et al*., 2002; Alzate *et al*., 2006; Boulet *et al*., 2006; Gorb *et al*., 2006; Yang *et al*., 2006; Snyder and Madura, 2008; Michaldova *et al*., 2011; Karataş *et al*., 2013). The chemical composition of the tunnel model with hydrogen saturated dangling bonds included 164 atoms and has the formula $Si_{40}Mg_6O_{54}H_{64}$. Since the real crystal structure of sepiolite includes two crystalline waters per Mg atom and several zeolitic waters, 12 crystalline and 8 zeolitic water molecules, were also included in the tunnel model and this increased the total number of atoms to 224. The crystalline water molecules are bonded to Mg^{2+} ions, whereas the zeolitic waters are located in the tunnels and form hydrogen bonds with the crystalline water molecules and with other zeolitic water molecules. The amount of zeolitic water can change with environmental relative humidity (Zhou *et al*., 2016). The zeolitic water can be easily removed upon thermal treatment at about 100ºC, whereas the crystalline water needs much more elevated temperatures (>350ºC) for removal (Ruiz-Hitzky, 2001).

The present study focussed on the penetration of 12 different organic molecules (Figure 2) into sepiolite tunnels. Among the compounds, pyridine (Sabah and Çelik, 2002), 2,2-bipyridyl (Sabah and Çelik, 2002), and Maya blue (indigo) (Ovarlez *et al*., 2009; Giustetto *et al*., 2010; Guistetto *et al*., 2011b; Martinez-Martinez *et al*., 2011) have been experimentally shown to access sepiolite tunnels. The long alkyl chains attached to organic molecules, such as DDAC, HTAC, SDBAC, TDEBAC, and lauric acid, were shortened in size to accelerate the computations. Among the organic molecules, DDAC, HTAC, methylene blue, SDBAC, and TDEBAC were considered in the cationic form.

In the present study, both the static and dynamic incorporation of organic molecules into sepiolite tunnels were investigated. Here, static adsorption implies that the organic molecules were initially placed inside the sepiolite tunnel and the whole system was relaxed (both in gas and COSMO (The Conductor-like Screening Model)) at Perdew–Burke-Ernzerhof (PBE) exchange-correlation (xc) functional with polarized triple-zeta basis set (TZVP). These optimized geometries were then employed to compute the corresponding interaction energies at the dispersion corrected Becke 97 xc functional (B97-D) with TZVP basis set. On the other hand, organic molecules were initially placed outside the tunnel for dynamic adsorption and were then gradually moved into sepiolite tunnels. The computational methodology applied for static incorporation of organic molecules into sepiolite tunnels was also employed to study dynamic incorporation. The static approach provides the best orientation of the organic molecules inside the tunnel, however, the dynamic approach helps to answer the following question: Can organic molecules really access sepiolite tunnels? Since water molecules are present at the entrance of sepiolite tunnels, the organic molecules might interact with water molecules and hinder further incorporation of the organic molecules into the interiors of tunnels. The dynamic mobility of the molecules was, therefore, verified to make certain judgments about the final positions of the organic

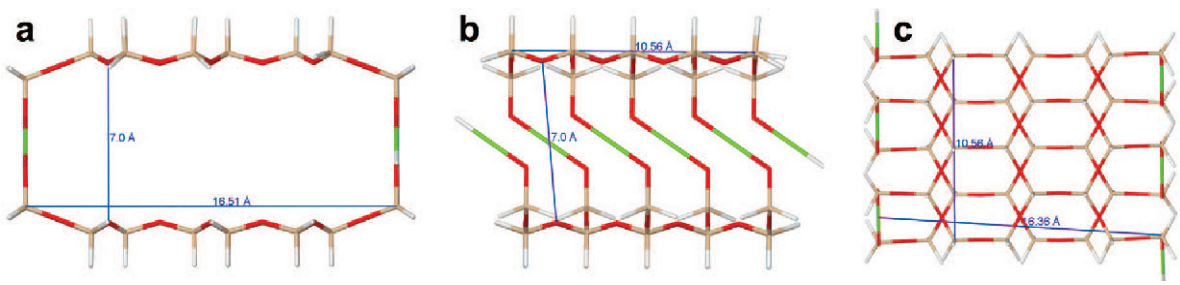

Figure 1. The front (a), side (b), and top (c) views of a sepiolite tunnel considered in this study with tunnel dimensions in Å.

https://doi.org/10.1346/CCMN.2016.064043 Published online by Cambridge University Press

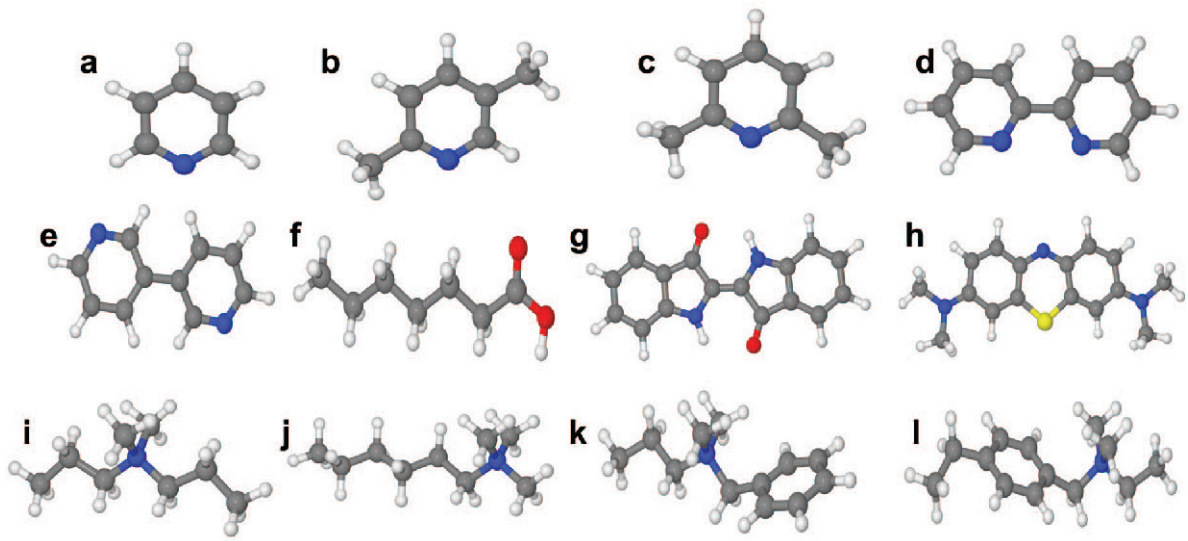

Figure 2. Organic compounds considered in this study: (a) pyridine, (b) 2,5-dimethylpyridine, (c) 2,6-dimethylpyridine, (d) 2,2-bipyridyl, (e), 3,3-bipyridyl, (f) lauric acid, (g) indigo, (h) methylene blue, (i) distearyldimethylammonium chloride DDAC, (j) hexadecyltrimethylammonium chloride HTAC, (k) stearyldimethylbenzylammonium chloride SDBAC, and (l) tetradecyl-dimetylethylbenzylammonium chloride TDEBAC.

molecules. Since only quantum chemistry calculations were considered in the present study rather than molecular dynamics, constructing a path for the dynamical motion was mandatory. By mimicking the nudged elastic band (NEB) method, Jónsson *et al*. (1998) found transition paths between the given initial and final states to construct a sequence of "images" of the system. In contrast to a standard NEB calculation, the organic molecule "images" in the present study were kept frozen to produce a sequence of images along the constructed path. Otherwise, a system image might simply transform into another orientation that is not along the desired path.

All geometry optimizations were performed using TURBOMOLE V6.1 (Ahlrichs *et al.*, 1989) quantum chemistry computer software package which uses density functional theory (DFT) with the Perdew, Burke, and Ernzerhof (PBE) (Perdue *et al*., 1996) functional and TZVP basis set. The PBE is similar to the other standard functionals like the Becke 3-term functional, Lee, Yang, Parr hybrid density functional (B3LYP), the Becke, Perdew xc functional (BP86), and the Tao, Perdew, Staroverov, and Scuseria xc functional (TPSS) predicts systematically expanded structures in comparison to the dispersion-corrected functionals (B97-D, long-range corrected hybrid density functional (wB97XD), Truhlar's meta-hybrid xc functional (MO6), and Truhlar's full local meta-hybrid xc functional (M06L)) (Minenkov *et al*., 2012). Because the adsorption configurations that resulted contained many atoms, the resolution of identity (RI) Eichkorn *et al*., 1995) approximation for all geometry optimizations was switched on and all atomic positions were relaxed except for the sepiolite cage. Subsequently, optimized geometries were used to calculate the interaction energies using the dispersion-corrected DFT functional (B97-D) employed using the TZVP basis set. The recent interaction energies obtained at the B97-D level between sepiolite and quaternary amine surfactants showed good agreement with the MP2, SCS-MP2, and the B2PLYP-D functionals (Karataş *et al.*, 2013). Only the B97-D was employed, however, for the calculation of interaction energies. The triple ζ basis set, TZVP, performed better than most of the 6-311G basis sets (Xu and Truhlar, 2011). In all interaction energy computations, water molecules were assumed to be a part of the sepiolite tunnel. Interaction energies were corrected against the basis set superposition error (BSSE) using the counterpoise (CP) method (Boys and Bernardi, 1970). The negative binding energies were obtained using the following formula:

$$E_{\mathrm{BE}}^{\mathrm{CP}} = E_{\mathrm{tunnel+comp}}^{(\mathrm{tunnel+comp})} - E_{\mathrm{tunnel}}^{(\mathrm{tunnel+comp})} + E_{\mathrm{comp}}^{(\mathrm{tunnel+comp})})$$

where $E_{\mathrm{BE}}^{\mathrm{CP}}$ is the CP corrected binding energy, $E_{\mathrm{tunnel+comp}}^{(\mathrm{tunnel+comp})}$, $E_{\mathrm{tunnel}}^{(\mathrm{tunnel+comp})}$, and $E_{\mathrm{comp}}^{(\mathrm{tunnel+comp})}$ the total energies of the compound+tunnel, tunnel, and the compound were calculated using the basis set of the complete system (tunnel+compound). Since a very limited number of zeolitic waters were included in the systems in comparison to the crystalline structure, the theoretical calculations were also performed by treating the remaining water molecules implicitly using the COSMO module of TURBOMOLE. The vacuum and COSMO optimized geometries at PBE/TZVP were employed in all B97-D/TZVP interaction energy computations considered in the present study.

https://doi.org/10.1346/CCMN.2016.064043 Published online by Cambridge University Press

RESULTS AND DISCUSSION

In both the static and dynamic computations, the sepiolite tunnel model was kept fixed to prevent any change in the crystalline structure of the sepiolite. Three different scenarios were carried out in the static case: (1) no water in the sepiolite tunnel, (2) the sepiolite tunnel with only crystalline water, and (3) the tunnel with both zeolitic and crystalline waters. In the dynamic case, however, only one model that included both zeolitic and crystalline waters was considered. In any case, the water molecules were allowed to relax if the system included water molecules.

Static incorporation of organic molecules into sepiolite tunnels

Sepiolite with crystalline and zeolitic waters. Below 120ºC (Ruiz-Hitzky, 2001), sepiolite accommodates both crystalline and zeolitic water molecules and, hence, the pore size of the tunnel is reduced. The models designed to study this system involved 12 crystalline and 8 zeolitic water molecules and all of the water molecules were allowed to relax in addition to the organic molecules. In particular, as each Mg atom was bound to two crystalline waters, four of the zeolitic waters were positioned on each side of the tunnel. The negative interaction energies computed at B97-D/TZVP (Table 1) for the relaxed structures at the PBE/TZVP level (Figure 3) revealed that the organic molecules exhibited the tendency to stay inside the tunnel. The major source of interaction was the electrostatic interactions that emerged between organic molecules and the oxygens of the water or the tunnel. Organic molecules, except for quaternary amines, form strong hydrogen bonds with zeolitic waters using an N (O)−H distance of 1.8−2.1 Å. In fact, the quaternary amines also formed hydrogen bonds with the oxygens of water and the sepiolite tunnels, but these hydrogen bonds have moderate forces due to the increased H−O distance of 2.17−2.60 Å. Both the gas phase and COSMO geometries were quite close to each other and, therefore, the interaction energies that resulted appeared almost similar (Table 1). Obviously, indigo was the most favorable molecule due to the formation of two strong hydrogen bonds with zeolitic waters (1.8 and 2.0 Å) and three other hydrogen bonds between the H of indigo and the O of water (2.28, 2.33, and 2.47 Å). Next to indigo was methylene blue, which formed several hydrogen bonds; four between the hydrogens of methylene blue and the oxygens of water with bond lengths of 2.25, 2.27, 2.29, and 2.42 Å and one hydrogen bond between the N of methylene blue and the H of water with a distance of 2.07 Å. Interestingly, 3,3-bipyridyl was found to be isoenergetic to methylene blue and formed two N−H bonds with lengths of 1.62 and 1.82 Å and several O-H bonds with a minimum bond length of 2.49 Å. The least stable complex arrangement inside a sepiolite tunnel was found for pyridine, which only had one N−H (1.75 Å) hydrogen bond and one O−H (2.29 Å) hydrogen bond.

Sepiolite with only crystalline water. A mild thermal treatment of around 120ºC (Ruiz-Hitzky, 2001) only eliminated the intracrystalline zeolitic water molecules in the sepiolite. As shown in the previous section, zeolitic water molecules played a key role in the stabilization of organic molecules inside the sepiolite tunnels by forming hydrogen bonds. The removal of zeolitic water molecules might, therefore, have substantial effects on the capacity of organic molecules to penetrate into the tunnels. In contrast to the above case that was based on the interaction energies (Table 2) of

Table 1. The counterpoise (CP) corrected and non-counterpoise corrected B97-D/TZVP interaction energies between sepiolite tunnels, which included crystalline and zeolitic water molecules and organic molecules calculated by employing PBE/TZVP structures relaxed at vacuum and COSMO.

Molecule	Interaction energy (kJ/mol)			
	Gas		COSMO	
	B97-D	B97-D (CP)	B97-D	B97-D (CP)
Pyridine	−120.66	−120.66	−122.70	−111.93
2,5-dimethylpyridine	−150.53	−133.62	−150.20	−133.21
2,6-dimethylpyridine	−130.43	−115.44	−129.97	−114.88
2,2-bipyridyl	−218.80	−198.17	−221.39	−200.92
3,3-bipyridyl	−255.49	−233.90	−258.11	−236.40
Lauric acid	−195.06	−175.25	−195.51	−175.54
Indigo	−267.25	−237.87	−239.41	−268.69
Methylene Blue	−269.69	−240.66	−265.05	−236.40
DDAC	−201.91	−180.75	−186.65	−165.25
HTAC	−154.50	−131.28	−148.94	−125.19
SDBAC	−241.45	−219.13	−232.05	−209.61
TDEBAC	−205.98	−179.27	−207.44	−181.47

https://doi.org/10.1346/CCMN.2016.064043 Published online by Cambridge University Press

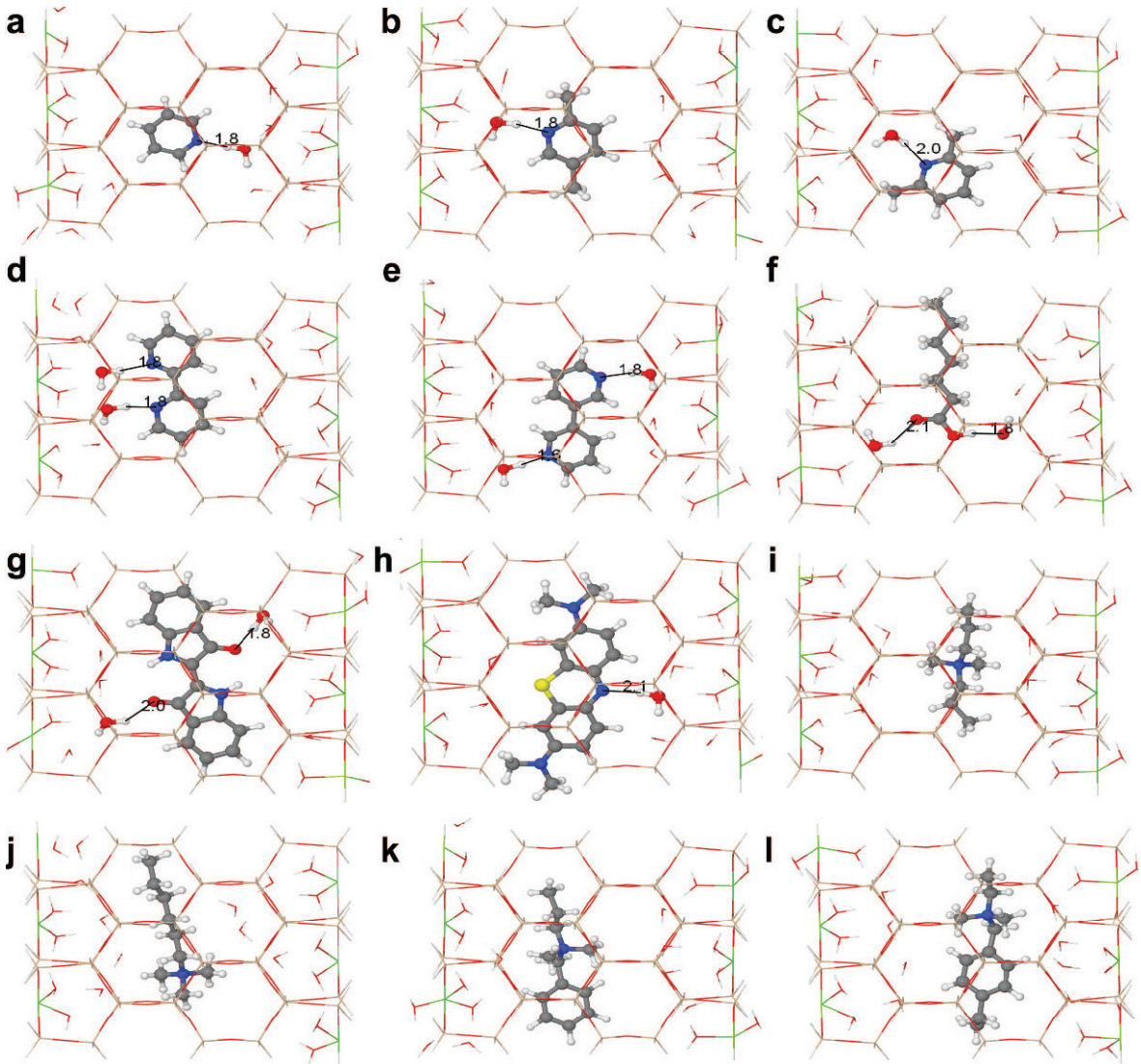

Figure 3. Relaxed structures of (a) pyridine, (b) 2,5-dimethylpyridine, (c) 2,6-dimethylpyridine, (d) 2,2-bipyridyl, (e), 3,3-bipyridyl, (f) lauric acid, (g) indigo, (h) methylene blue, (i) distearyldimethylammonium chloride DDAC, (j) hexadecyltrimethylammonium chloride HTAC, (k) stearyldimethylbenzylammonium chloride SDBAC, and (l) tetradecyldimethylethylbenzylammonium chloride TDEBAC (in COSMO model) inside a sepiolite tunnel with crystalline and zeolitic water molecules with hydrogen bond distances in Å. The different elements were represented by the colors: H, white/white grayscale; C, gray/gray grayscale; N, blue/black grayscale; O, red/black grayscale; Si, melon yellow/light gray grayscale; and Mg, green/light gray grayscale.

relaxed structures (Figure 4), the strongest binding to the sepiolite cage was found with methylene blue. This was due to the formation of several hydrogen bonds between methylene blue and crystalline water molecules; three hydrogen bonds with a distance 2.4–2.8 Å between the H of methylene blue and the O of water, and the one hydrogen bond between the N of methylene blue and the H of water with a distance of 2.0 Å. The CP-corrected interaction energy for methylene blue in the presence of only crystalline water was 6.88 kJ/mol higher than the case with both crystalline and zeolitic water. Binding energies for indigo and 2,2-bipyridyl were isoenergetic and were higher than methylene blue by approximately 35 kJ/mol. Similar to the case with both crystalline and zeolitic water, pyridine had the least stable complex. In particular, due to the exclusion of zeolitic waters, pyridine got close to the edge of the tunnel where it formed two hydrogen bonds (2.11 and 2.22 Å) with the crystalline waters of the tunnel. In general, the binding energies were notably reduced when the tunnel only contained the crystalline water in comparison to the case with both crystalline and zeolitic water except for the

https://doi.org/10.1346/CCMN.2016.064043 Published online by Cambridge University Press

Table 2. The counterpoise (CP) corrected and non-counterpoise corrected B97-D/TZVP interaction energies between sepiolite tunnels (which included only crystalline water molecules) and organic molecules calculated by employing PBE/TZVP structures relaxed at vacuum and COSMO.

Molecule	Interaction energy (kJ/mol)			
	Gas		COSMO	
	B97-D	B97-D (CP)	B97-D	B97-D (CP)
Pyridine	−100.78	−88.41	−100.76	−88.13
2,5-dimethylpyridine	−140.31	−124.80	−140.95	−125.66
2,6-dimethylpyridine	−155.97	−139.85	−155.01	−139.00
2,2-bipyridyl	−210.11	−189.73	−215.02	−194.66
3,3-bipyridyl	−192.38	−174.89	−189.54	−172.19
Lauric acid	−150.63	−133.14	−150.73	−133.39
Indigo	−222.57	−197.26	−219.55	−194.26
Methylene Blue	−250.03	−223.19	−256.33	−229.52
DDAC	−186.04	−164.19	−178.53	−157.36
HTAC	−175.49	−155.31	−175.38	−155.16
SDBAC	−182.48	−160.27	−178.75	−156.96
TDEBAC	−187.42	−164.78	−185.37	−162.78

2,6-dimethylpyridine and HTAC molecules. More specifically, these two molecules exhibited lower energy than both the crystalline and zeolitic water case by 24.12 and 29.97 kJ/mol, respectively. This energy gain was due to the formation of much stronger hydrogen bonds. For example, the hydrogen bond distance between the N of 2,6-dimethylpyridine and the H of water decreased from 1.95 Å to 1.79 Å.

Anhydrous sepiolite. If sepiolite is heated above 250ºC (Ruiz-Hitzky, 2001), it loses both the crystalline and zeolitic waters. To mimic this condition, a sepiolite tunnel was constructed without any water molecules. Organic molecules were initially placed inside the sepiolite tunnel and the whole system was relaxed (both in the gas phase and COSMO) at PBE/TZVP. These optimized geometries were then employed to compute the corresponding interaction energies at the B97-D/TZVP level of theory. The resulting interaction energies (Table 3) and geometries (Figure 5) revealed that the interaction energies obtained from both the gas phase and COSMO were quite close to each other and the CP-corrected energies were higher than the non-corrected energies by at least 20 kJ/mol. In both the gas phase and COSMO media, all the interaction energies were negative, which implies that all organic molecules tended to stay inside the sepiolite tunnel. In the gas phase orientations, methylene blue had the lowest CP-corrected interaction energy followed by indigo, which was 14.89 kJ/mol higher in energy than methylene blue. In contrast, indigo had the lowest energy structure in the COSMO model with an interaction energy of only

Table 3. The counterpoise (CP) corrected and non-counterpoise corrected B97-D/TZVP interaction energies between sepiolite tunnels (without crystalline or zeolitic water molecules) and organic molecules calculated by employing PBE/TZVP structures relaxed at vacuum and COSMO.

Molecule	Interaction energy (kJ/mol)			
	Gas		COSMO	
	B97-D	B97-D (CP)	B97-D	B97-D (CP)
Pyridine	−175.86	−159.22	−175.72	−159.09
2,5-dimethylpyridine	−199.78	−177.55	−199.98	−177.67
2,6-dimethylpyridine	−160.06	−138.56	−160.2	−138.60
2,2-bipyridyl	−185.18	-158.41	-185.26	−158.31
3,3-bipyridyl	−224.36	−200.64	−224.86	−201.04
Lauric acid	−128.37	−108.32	−127.82	−107.93
Indigo	−231.78	−200.24	−246.48	−216.70
Methylene Blue	−250.62	−215.13	−251.11	−215.34
DDAC	−133.94	−113.92	−134.44	−114.36
HTAC	−154.50	−130.63	−155.52	−131.60
SDBAC	−153.64	−130.89	−154.09	−131.31
TDEBAC	−156.66	−133.48	−157.69	−133.26

https://doi.org/10.1346/CCMN.2016.064043 Published online by Cambridge University Press

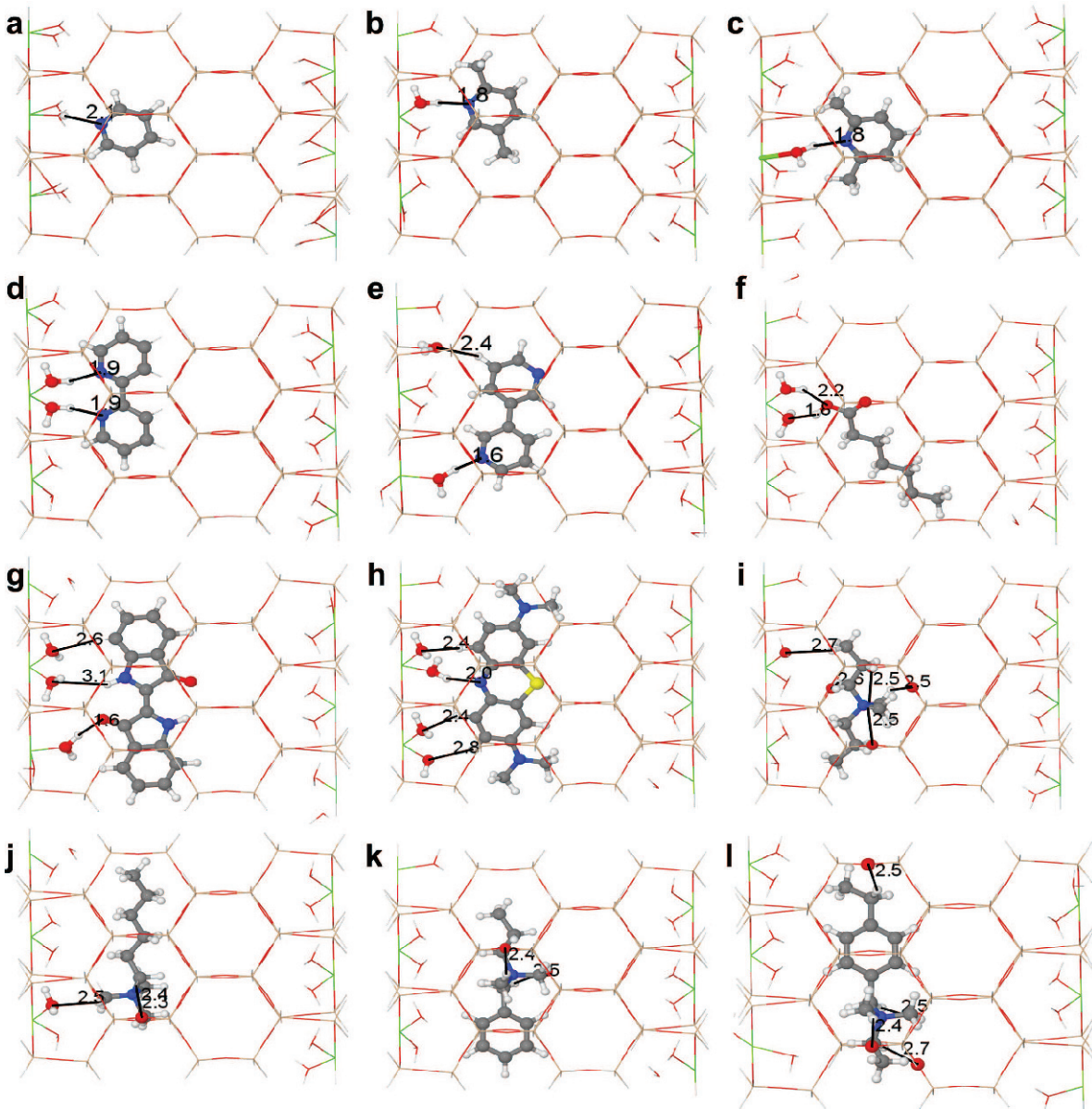

Figure 4. Relaxed structures of (a) pyridine, (b) 2,5-dimethylpyridine, (c) 2,6-dimethylpyridine, (d) 2,2-bipyridyl, (e), 3,3-bipyridyl, (f) lauric acid, (g) indigo, (h) methylene blue, (i) distearyldimethylammonium chloride DDAC, (j) hexadecyltrimethylammonium chloride HTAC, (k) stearyldimethylbenzylammonium chloride SDBAC, and (l) tetradecyldimetylethylbenzylammonium chloride TDEBAC (in COSMO model) inside a sepiolite tunnel with only crystalline waters with hydrogen bond distances in Å. The different elements were represented by the colors: H, white/white grayscale; C, gray/gray grayscale; N, blue/black grayscale; O, red/black grayscale; Si, melon yellow/light gray grayscale; Mg, green/light grayscale.

1.36 kJ/mol lower than methylene blue. The optimized structures (Figure 5) revealed that the interactions that occurred between Mg and either the O or the N of the organic molecule were quite important for stabilization of the systems. Thus, the corresponding interaction energies of these systems were reasonably lower (at most, approximately 100 kJ/mol) than the molecules that contained quaternary amines. In particular, the Mg–N (O) distances were between 2.1 and 3.3 Å. In the case of systems with quaternary amines, hydrogen bonds (2.24–2.45 Å) between the H of the organic molecule and the O of sepiolite were responsible for the interactions. In addition, the Mg–N (O) and hydrogen bond distances were almost identical in the gas phase and COSMO model geometries. The fact that no significant change in the interaction energies (Table 3) for the gas and the COSMO model orientations was noted also supports this interpretation.

https://doi.org/10.1346/CCMN.2016.064043 Published online by Cambridge University Press

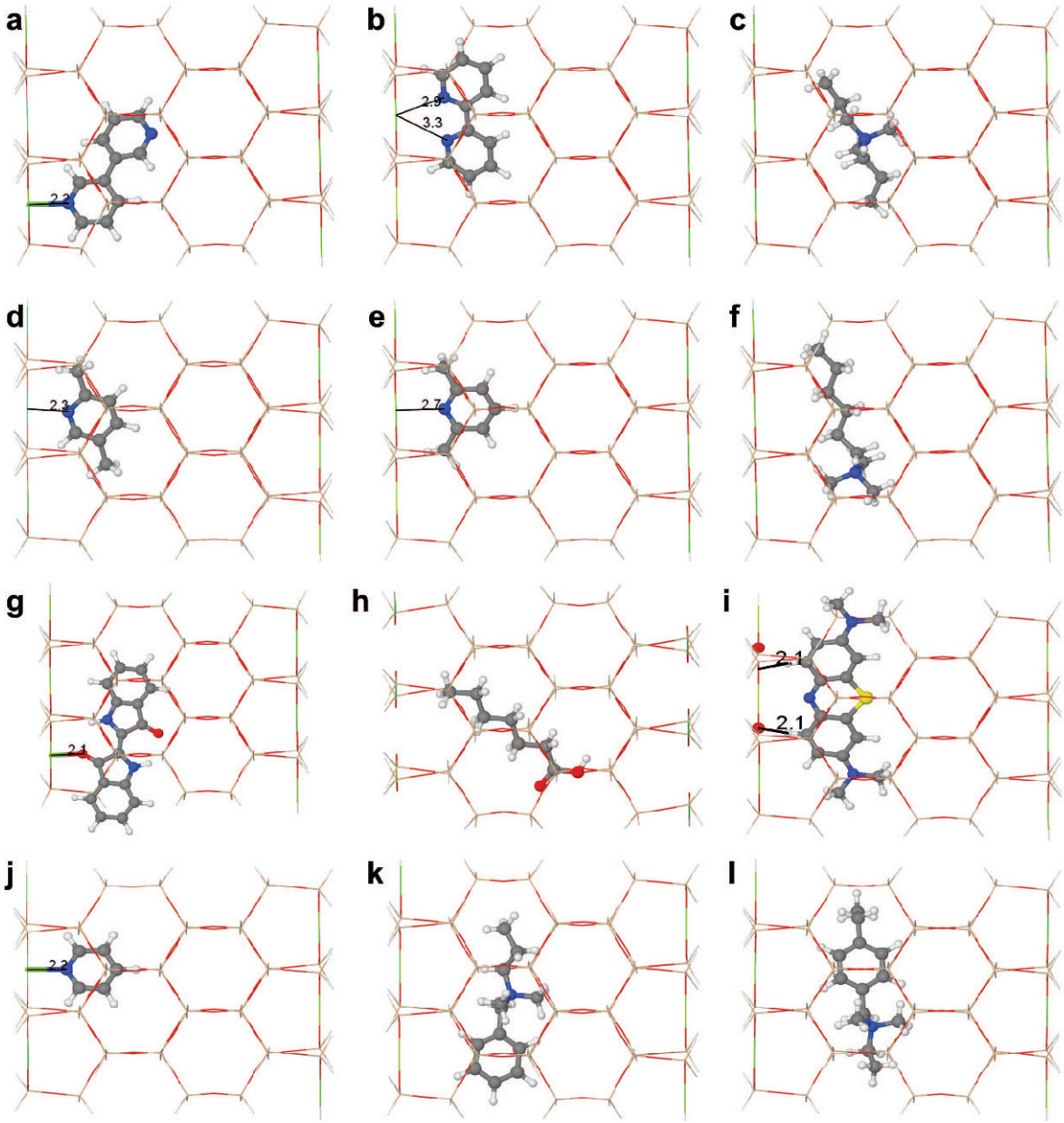

Figure 5. Relaxed structures of (a) 3,3-bipyridyl, (b) 2,2-bipyridyl, (c) distearyldimethylammonium chloride DDAC, (d) 2,5-dimethylpyridine, (e) 2,6-dimethylpyridine, (f) hexadecyltrimethylammonium chloride HTAC, (g) indigo, (h) lauric acid, (i) methylene blue, (j) pyridine, (k) stearyldimethylbenzylammonium chloride SDBAC, and (l) tetradecyldimetylethylbenzyl-ammonium chloride TDEBAC inside a sepiolite tunnel with hydrogen bond distances in Å. The different elements were represented by the colors: H, white; C, gray/gray grayscale; N, blue/black grayscale; O, red/black grayscale; Si, melon yellow/light gray grayscale; Mg, green/light gray grayscale.

The tunnel structure used to model anhydrous sepiolite does not reflect the actual tunnel at elevated temperatures (>350ºC) because the tunnels are folded and the pore size is drastically reduced at that temperature in comparison to the hydrated sepiolite. In particular in the folded tunnel structure, the closest Si−Si distance became approximately 4.5 Å in comparison to 8.1 Å in the unfolded structure. Experiments showed that even Ar atoms cannot penetrate into these narrow sepiolite pores (Ruiz-Hitzky, 2001). This suggests that none of the organic molecules considered in the present study can gain access to these folded tunnels, too.

Dynamic incorporation of organic molecules into sepiolite tunnels

Until now, all the organic molecules were initially placed inside a sepiolite tunnel and whether these

https://doi.org/10.1346/CCMN.2016.064043 Published online by Cambridge University Press

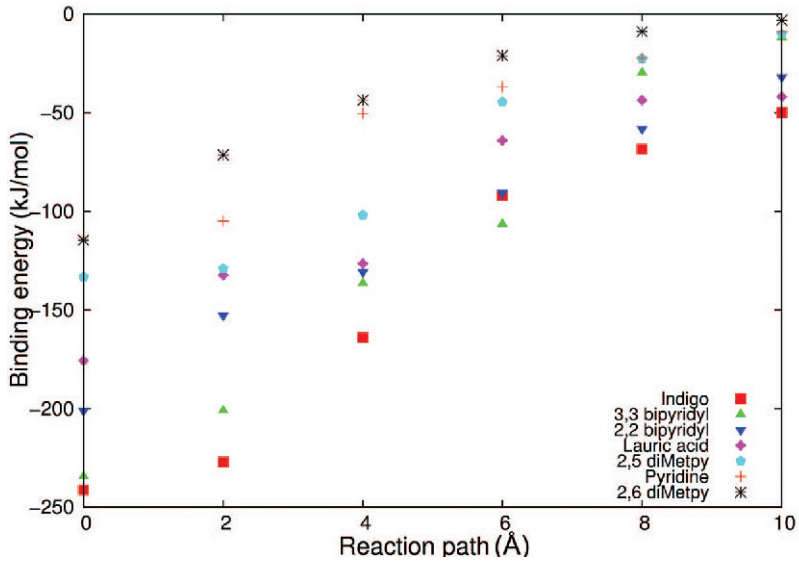

Figure 6. Binding energies as a function of the reaction path for organic compounds 2,5-dimethylpyridine, 2,6-dimethylpyridine, indigo, lauric acid, 2,2-bipyridyl, 3,3-bipyridyl, and pyridine.

molecules tended to stay inside the tunnel with or without water was observed. All these optimized structures can be assumed to be the final positions of organic compounds, if the compounds manage to penetrate inside the tunnel. Therefore, these calculations are not completely adequate to clarify the incorporation of organic compounds into sepiolite tunnels. At this stage, finding the pathway an organic molecule takes from outside the tunnel until it is inside the tunnel is necessary. Here, the orientation of the sepiolite cage and the organic compound were fixed and only water molecules were allowed to relax. The optimized structures reported in *Sepiolite with crystalline and zeolitic waters* were assumed to be the last frame of reaction path zero in Figure 6 and the orientation of the organic molecule in this frame was also employed for the other frames. In total, five frames were used to construct the travel path of the organic compound and the frame of each organic molecule as it was moved by 2 Å to the outside of the tunnel. This eventually gave a route with a 10 Å length. The neutral molecule results (Figure 6) indicated that the binding energy was lowered when the reaction path was changed from 10 Å to 0 Å for all molecules. This strongly indicated that no barrier prevented the access of molecules to the tunnel. The snapshots (Figure 7) of indigo adsorbed to sepiolite indicated that the number of hydrogen bonds increased when the reaction path was decreased. Similar snapshots were also obtained for the remaining neutral molecules (Figure 6). In particular, only one hydrogen bond with one zeolitic water molecule with a distance of 2.4 Å was formed when the reaction path equalled 10 Å. This zeolitic water can further create three additional hydrogen bonds with the neighboring water molecules with distances of 1.48, 1.75, and 1.80 Å. All zeolitic water molecules were located close to the sepiolite crystalline water molecules and, hence, a significant change in the positions of the zeolitic water molecules was not observed. These results suggest that all of these organic molecules tend to gain access to sepiolite tunnels, which supports the experimental studies of Ovarlez *et al.* (2009) and Sabah and Çelik (2002) in regard to pyridine, indigo, and 2,2-bipyridyl. On the other hand, Ruiz-Hitzky (2001) stated that 2,6-dimethylpyridine molecules cannot penetrate into the tunnels and instead were mostly located in the channels. In order to verify the most preferable adsorption site for 2,6-dimethylpyridine, a channel was also built starting from the tunnel structure (Figure 8). The binding energy computations performed at B97-D/TZVP level of theory showed that the interaction energy was only −72.36 kJ/mol when 2,6-dimethylpyridine was placed in a sepiolite channel. In the structure of this silica layer, a hydrogen bond (1.7 Å) and the non-planar 2,6-dimethylpyridine molecule are present. However, 2,6-dimethylpyridine adsorption in the tunnel lowers the interaction energy by 42.52 kJ/mol in comparison to adsorption in the channel. This energy gain was probably due to the formation of an additional hydrogen bond (2.2 and 2.0 Å). Hence, these findings contradict the results of Ruiz-Hitzky (2001). However, if 2,6-dimethylpyridine favored an orientation inside the sepiolite channel that included more than one hydrogen bond, then expecting similar interaction energies in both sepiolite channels and tunnels would be reasonable.

The dynamic incorporation of the cationic molecules DDAC, HTAC, SDBAC, TDEBAC, and methylene blue into sepiolite (Figure 9) indicated that only methylene blue reacted similarly to the neutral molecules with a lower binding energy with a decrease in the reaction

https://doi.org/10.1346/CCMN.2016.064043 Published online by Cambridge University Press

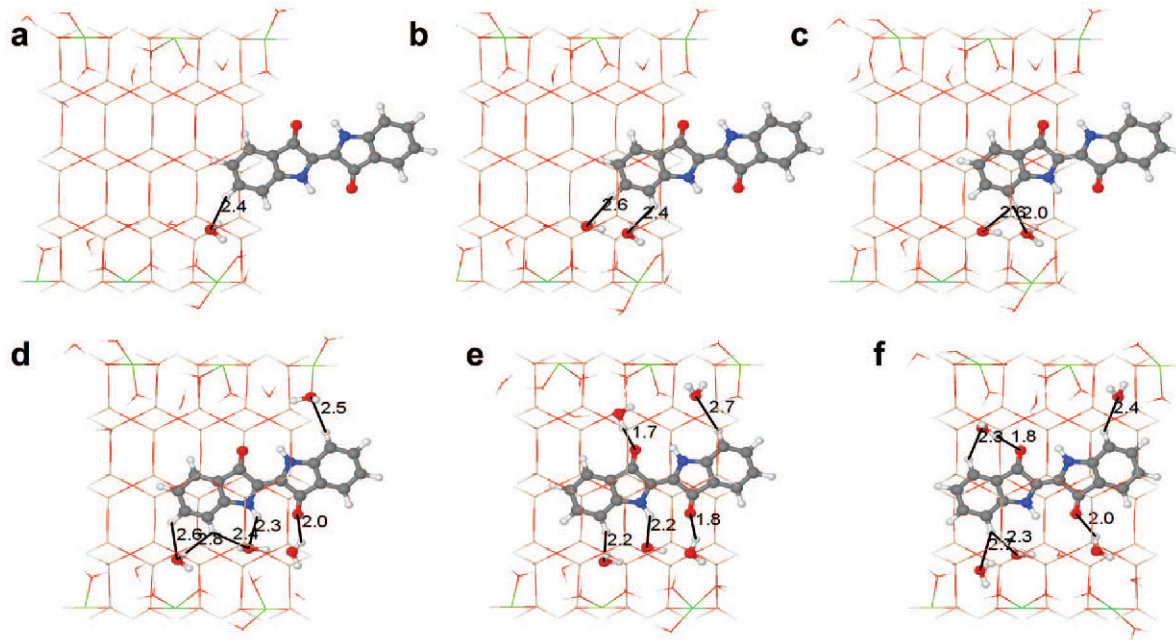

Figure 7. Snapshots of the structures of a sepiolite tunnel with adsorbed indigo at reaction paths of (a) 10 Å, (b) 8 Å, (c) 6 Å, (d) 4 Å, (e) 2 Å, and (f) 0 Å, with hydrogen bond distances in Å.

path. This agrees with the experimental findings of Ruiz-Hitzky (2001). In contrast to methylene blue, other molecules that contain a quaternary amine do not prefer to be located completely inside the tunnels. More specifically, the binding energy first started to decrease with a decrease in the reaction path to 6 Å and then increased for DDAC. The difference in the binding energy for 4 and 6 Å reaction paths was almost 54 kJ/mol. The reason for the increased binding energy for the 4 Å reaction path was the close contact (2.18 Å) between a H atom in DDAC and a Si atom of the cage. This phenomenon was also true for the other cationic molecules: An increase in the binding energy was due to undesirable electrostatic interactions between the cage and the organic molecules. The close contacts between the H atoms of DDAC, HTAC, SDBAC, and TDEBAC and the Si of the sepiolite cage were unavoidable due to the restrictions (the organic molecule position was not allowed to change) imposed in the computational setup (Table 4). However, the settlement of H atoms of organic molecules to energetically more favorable positions was expected if the molecules were free to move like the reaction path at 0 Å. Therefore, a reasonable conclusion to draw was, "these cationic molecules might also tend to gain access to sepiolite tunnels."

Only zeolitic and crystalline water molecules in sepiolite were included in the dynamic incorporation scenario. However, external water molecules would be present in an aqueous environment, especially at pore openings. Eight additional water molecules were added to the sepiolite model to investigate the effect of the external water molecules on the binding energies. These calculations were carried out by only considering the

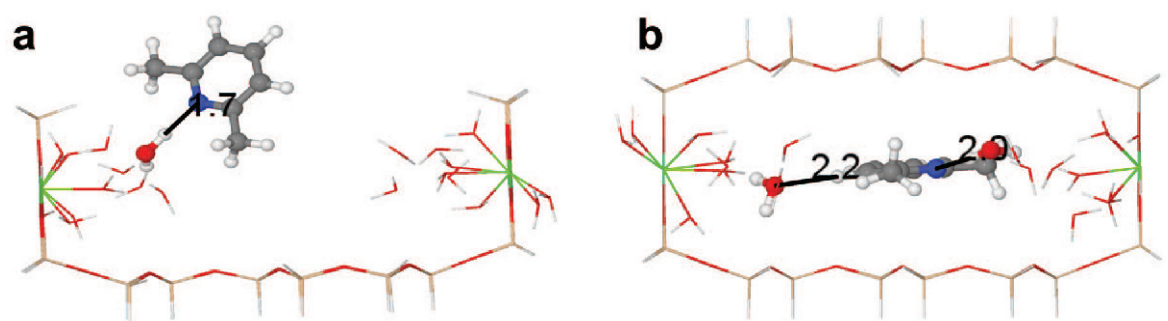

Figure 8. A 2,6-dimethyl-pyridine molecule (a, left) in sepiolite channel and (b, right) in sepiolite tunnel, with hydrogen bond distances in Å.

https://doi.org/10.1346/CCMN.2016.064043 Published online by Cambridge University Press

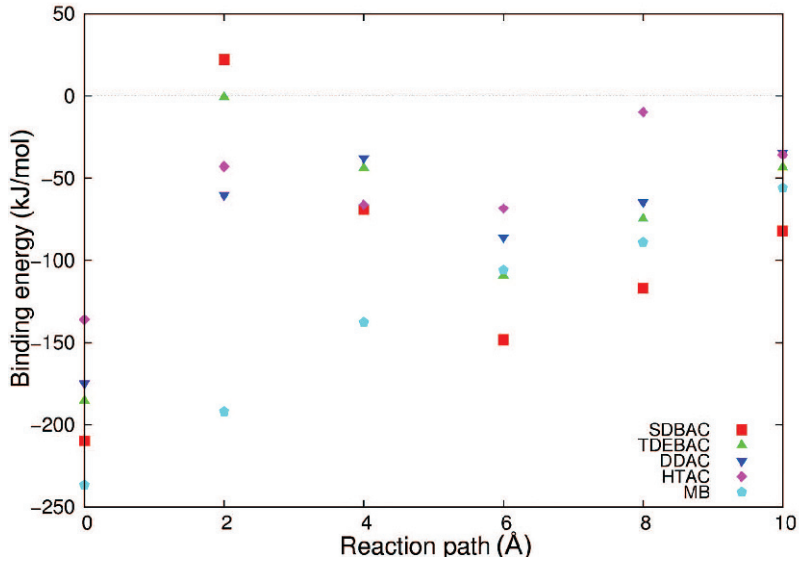

Figure 9. Binding energies as a function of reaction path for the organic molecules DDAC, HTAC, SDBAC, TDEBAC, and methylene blue (MB).

smallest organic molecule, pyridine. The snapshots (Figure 10) showed that additional external water molecules at first covered the pore openings entirely. After pyridine moved inward to the hydrogen bonds between the external water molecules, the hydrogen bonds started to break and allowed pyridine to move into the tunnel. Finally, when pyridine moved deep into the tunnel, external waters completely closed the mouth of the pore again. The calculated binding energies (Table 5) of these orientations indicated that an energy barrier evolved at reaction path 6 Å. The increased binding energy at reaction path 6 Å suggests that external water molecules preferred to stay together and form hydrogen bonds. When pyridine reached to the center of a tunnel, fully hydrogen bonded external water molecules appeared again in the tunnel opening and a substantial reduction in the binding energy occurred with energies almost similar in comparison to the case of only crystalline and zeolitic water. These findings suggest that, if external water molecules are present in the pore opening, organic molecules cannot readily access sepiolite tunnels.

CONCLUSIONS

The present study aimed to clarify the incorporation of twelve different organic molecules into the tunnels of sepiolite using density functional theory computations. At first, organic molecules were directly positioned inside the tunnel. The binding energy computations show that all of the organic molecules preferred a location inside sepiolite tunnels. In particular, indigo was found to be the most favored molecule inside sepiolite tunnels that contained both crystalline and zeolitic water molecules. When sepiolite contained only crystalline water, methylene blue formed the strongest hydrogen bonds with the water molecules of the tunnel. If all water molecules were removed from a sepiolite tunnel, indigo became the most energetically promising molecule by forming a strong Mg–O coordination.

Table 4. Distances between the closest two Si and H atoms with the shortest lengths for each quaternary ammonium compound in bold print.

Reaction path (Å)	DDAC	HTAC	SDBAC	TDBAC
0	2.48, 2.70	2.63, 2.68	2.61, 2.83	2.52, 2.70
2	2.38, 2.48	**2.14**, 2.48	**2.12**, 2.27	**2.02**, 2.28
4	**2.18**, 2.77	2.53, 2.58	2.46, 2.62	2.46, 2.65
6	2.59, 2.70	2.52, 2.63	2.49, 2.87	2.68, 3.03
8	2.78, 2.99	**2.26**, 2.35	2.47, 3.21	2.57, 2.81
10	3.06, 3.14	2.76, 3.08	3.39, 3.74	2.84, 2.87

https://doi.org/10.1346/CCMN.2016.064043 Published online by Cambridge University Press

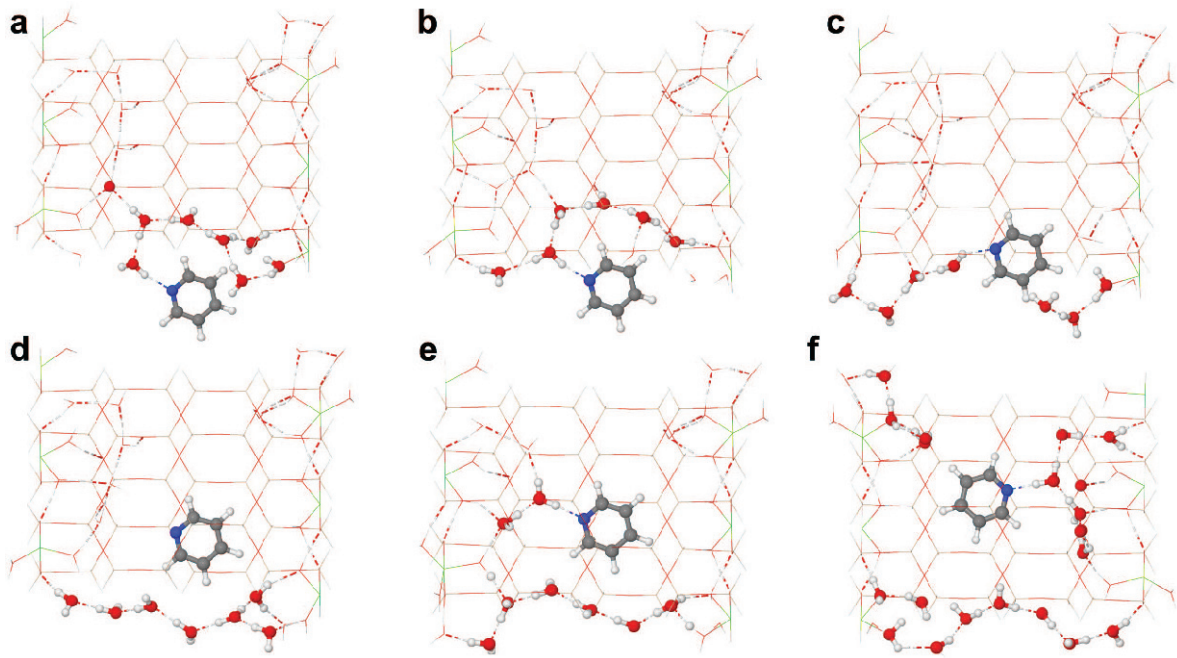

Figure 10. Snapshots of the structures of sepiolite tunnel (including eight external water molecules) with adsorbed pyridine at reaction paths of (a) 10 Å, (b) 8 Å, (c) 6 Å, (d) 4 Å, (e) 2 Å, and (f) 0 Å, with hydrogen bond distances shown by dashed lines.

These results are completely in agreement with experimental findings about pyridine, indigo, 2,2-bipyridyl, and methylene blue. In addition to these calculations, the dynamic motion of organic molecules was also investigated to show whether any of these organic molecules can travel to the inside of sepiolite tunnels without facing any barrier. For this purpose, a path with a length of 10 Å was found to be satisfactory and organic molecules were only allowed to translate along one axis and rotational motion was prohibited. Pseudo barriers exist for 3D cationic molecules due to the inconvenient electrostatic interactions between the hydrogens of organic molecules and the silicons of sepiolite tunnels, which were caused by the fixed coordinates used for the organic molecules. If these molecules were allowed to change coordinates (as in the final images), these repelling interactions would not have been observed. These findings indicate, therefore, that all organic molecules considered in the present study might gain access to sepiolite tunnels. On the other hand, if external water molecules are present in sepiolite tunnel openings, the water molecules tend to block the entry of organic molecules.

ACKNOWLEDGMENTS

Computing resources were provided by the National Centre for High Performance Computing of Turkey (UHEM), under Grant Number 1002132012, TÜBİTAK

Table 5. The counterpoise (CP) corrected and non-counterpoise corrected B97-D/TZVP interaction energies between sepiolite tunnels (including external water molecules) and pyridine calculated by employing PBE/TZVP structures relaxed at vacuum and COSMO.

	Interaction energy (kJ/mol)			
	Gas		COSMO	
Reaction path (Å)	B97-D	B97-D (CP)	B97-D	B97-D (CP)
0	−126.50	−115.41	−129.37	−117.97
2	−131.57	−119.97	−129.05	−117.06
4	−77.77	−67.39	−76.77	−65.91
6	−70.23	−58.76	−67.54	−56.01
8	−87.85	−78.88	−85.72	−76.03
10	−72.93	−64.86	−71.02	−62.66

https://doi.org/10.1346/CCMN.2016.064043 Published online by Cambridge University Press

ULAKBİM, High Performance, and Grid Computing Centre (TRUBA resources) and Informatics Institute of Istanbul Technical University.

REFERENCES

Ahlrichs, R., Bär, M., Häser, M., Horn, H., and Kölmel, C. (1989) Electronic structure calculations on workstation computers: The program system turbomole. *Chemical Physics Letters*, **162**, 165–169.

Alvarado, M., Jr., Chianelli, R.C., and Arrowood, R.M. (2012) Computational study of the structure of a sepiolite/thioindigo Mayan pigment. *Bioinorganic Chemistry and Applications*, **2012**, 672562.

Alzate, L.F., Ramos, C.M., Hernandez, N.M., Hernandez, S.P., and Mina, N. (2006) The vibrational spectroscopic signature of tnt in clay minerals. *Vibrational Spectroscopy*, **42**, 357–368.

Boulet, P., Greenwell, H.C., Stackhouse, S., and Coveney, P.V. (2006) Recent advances in understanding the structure and reactivity of clays using electronic structure calculations. *Journal of Molecular Structure-Theochem*, **762**, 33–48.

Boys, S.F. and Bernardi, F. (1970) The calculation of small molecular interactions by the differences of separate total energies. Some procedures with reduced errors. *Molecular Physics*, **19**, 553.

Chatterjee, A., Iwasaki, T., Ebina, T., and Hayashi, H. (1997) Quantum chemical calculation on clay-water interface. *Applied Surface Science*, **121**, 167–170.

Chatterjee, A., Iwasaki, T., Ebina, T., and Miyamoto, A. (1999) A dft study on clay–cation–water interaction in montmorillonite and beidellite. *Computational Materials Science*, **14**, 119–124.

Davis, M.E. (2002) Ordered porous materials for emerging applications. *Nature*, **417**, 813–821.

Eichkorn, K., Treutler, O., Öhm, H., Häser, M., and Ahlrichs, R. (1995) Auxiliary basis sets to approximate coulomb potentials. *Chemical Physics Letters*, **242**, 652–660.

Giustetto, R., Levy, D., Wahyudi, O., Ricchiardi, G., and Vitillo, J.G. (2011a) Crystal structure refinement of a sepiolite/indigo Maya blue pigment using molecular modelling and synchrotron diffraction. *European Journal of Mineralogy*, **23**, 449–466.

Giustetto, R., Seenivasan, K., Bonino, F., Ricchiardi, G., Bordiga, S., Chierotti, M.R., and Gobetto, R. (2011b) Host/guest interactions in a sepiolite-based Maya blue pigment: A spectroscopic study. *Journal of Physical Chemistry C*, **115**, 16764–16776.

Giustetto, R., Seenivasan, K., and Bordiga, S. (2010) Spectroscopic characterization of a sepiolite based Maya blue pigment. *Periodico di Mineralogia*, **Special Issue**, 21–37.

Gorb, L., Lutchyn, R., Zub, Y., Leszczynska, D., and Leszczynski, J. (2006) The origin of the interaction of 1,3,5-trinitrobenzene with siloxane surface of clay minerals. *Journal of Molecular Structure-Theochem*, **766**, 151–157.

Jónsson, H., Mills, G., and Jacobsen, K.W. (1998) Nudged elastic band method for finding minimum energy paths of transitions, in classical and quantum dynamics in condensed phase simulations. Pp. 385–404 in *Classical and Quantum Dynamics in Condensed Phase Simulations* (B.J. Berne, G. Ciccotti, and D.F. Coker, editors). World Scientific Publishing.

Karataş, D., Tekin, A., and Çelik, M.S. (2013) Adsorption of quaternary amine surfactants and their penetration into the intracrystalline cavities of sepiolite. *New Journal of Chemistry*, **37**, 3936–3948.

Kuang, W.X., Facey, G.A., and Detellier, C. (2006) Organo-mineral nanohybrids. Incorporation, coordination and structuration role of acetone molecules in the tunnels of sepiolite. *Journal of Materials Chemistry*, **16**, 179–185.

Mammeri, F., Bourhis, E.L., Rozes, L., and Sanchez, C. (2005) Mechanical properties of hybrid organic–inorganic materials. *Journal of Materials Chemistry*, **15**, 3787.

Martinez-Martinez, V., Corcostegui, C., Prieto, J.B., Gartzia, L., Salleres, S., and Arbeloa, I.L. (2011) Distribution and orientation study of dyes intercalated into single sepiolite fibers. A confocal fluorescence microscopy approach. *Journal of Materials Chemistry*, **21**, 269–276.

Mehdi, A., Reye, C., and Corriu, R. (2011) From molecular chemistry to hybrid nanomaterials. Design and functionalization. *Chemical Society Reviews*, **40**, 563–574.

Michalkova, A., Robinson, T.L., and Leszczynski, J. (2011) Adsorption of thymine and uracil on 1:1 clay mineral surfaces: Comprehensive ab initio study on influence of sodium cation and water. *Physical Chemistry Chemical Physics*, **13**, 7862–7881.

Minenkov, Y., Singstad, A., Occhipinti, G., and Jensen, V.R. (2012) The accuracy of dft-optimized geometries of functional transition metal compounds: A validation study of catalysts for olefin metathesis and other reactions in the homogeneous phase. *Dalton Transactions*, **41**, 5526–5541.

Ovarlez, S., Giulieri, F., Chaze, A.M., Delamare, F., Raya, J., and Hirschinger, J. (2009) The incorporation of indigo molecules in sepiolite tunnels. *Chemistry A European Journal*, **15**, 11326–11332.

Perdew, J.P., Burke, K., and Ernzerhof, M. (1996) Generalized gradient approximation made simple. *Physical Review Letters*, **77**, 3865.

Post, J.E., Bish, D.L., and Heaney, P.J. (2007) Synchrotron powder X-ray diffraction study of the structure and dehydration behavior of sepiolite. *American Mineralogist*, **92**, 91–97.

Ruiz-Hitzky, E. (2001) Molecular access to intracrystalline tunnels of sepiolite. *Journal of Materials Chemistry*, **11**, 86–91.

Sabah, E. and Çelik, M.S. (2002) Interaction of pyridine derivatives with sepiolite. *Journal of Colloid and Interface Science*, **251**, 33–38.

Snyder, J.A. and Madura, J.D. (2008) Interaction of the phospholipid head group with representative quartz and aluminosilicate structures: An ab initio study. *Journal of Physical Chemistry B*, **112**, 7095–7103.

Tunega, D., Haberhauer, G., Gerzabek, M.H., and Lischka, H. (2002) Theoretical study of adsorption sites on the (001) surfaces of 1:1 clay minerals. *Langmuir*, **18**, 139–147.

Xu, X. and Truhlar, D.G. (2011) Accuracy of effective core potentials and basis sets for density functional calculations, including relativistic effects, as illustrated by calculations on arsenic compounds. *Journal of Chemical Theory and Computation*, **7**, 2766–2779.

Yang, T., Wen, X.D., Li, J.F., and Yang, L.M. (2006) Theoretical and experimental investigations on the structures of purified clay and acid-activated clay. *Applied Surface Science*, **252**, 6154–6161.

Zhou, J., Lu, X., and Boek, E.S. (2016) Confined water in tunnel nanopores of sepiolite: Insights from molecular simulations. *American Mineralogist*, **101**, 713-718.

(*Received 3 August 2016; revised 13 December 2016; Ms. 1125; AE: A. Kalinichev*)